Hydrothermal synthesis of 3D cauliflower anatase TiO2 and bio sourced activated carbon: adsorption and photocatalytic activity in real water matrices

El Mountassir El Mouchtari, Lekbira El Mersly, Oussama Jhabli, Hafid Anane, Anne Piram, Samir Briche, Pascal Wong-Wah-Chung, Salah Rafqah

Hydrothermal synthesis of 3D cauliflower anatase TiO_2 and bio sourced activated carbon: adsorption and photocatalytic activity in real water matrices

El Mountassir El Mouchtari [1,2*], Lekbira El Mersly[1], Oussama Jhabli[3], Hafid Anane [1], Anne Piram [2], Samir Briche [3], Pascal Wong-Wah-Chung[2], Salah Rafqah[1*]

[1] LCAM, Faculté Polydisciplinaire de Safi, Université Cadi Ayyad, Morocco.

[2] Aix-Marseille Univ, CNRS, LCE, Marseille, France.

[3] Département Stockage de l'Energie et Revêtements Multifonctionnels (SERM), MAScIR,

***Corresponding authors :**

El Mountassir El Mouchtari : Laboratoire de Chimie Analytique et Moléculaire (LCAM) - Département de Chimie - Faculté polydisciplinaire de Safi - Université Cadi Ayyad - Morocco

Aix-Marseille Université - Europole de l'Arbois -bat. Villemin – BP80 - 13545 Aix-en-Provence- France Tel: 00 33 7 53 44 51 58

Email: elmountassirelmouchtari@gmail.com

Salah RAFQAH : Laboratoire de Chimie Analytique et Moléculaire (LCAM) - Département de Chimie - Faculté polydisciplinaire de Safi - Université Cadi Ayyad - Morocco

Tel : 00-212-524669357 ; Fax : 00-212-524669516.

E-mail : rafqah@gmail.com

Graphical abstract

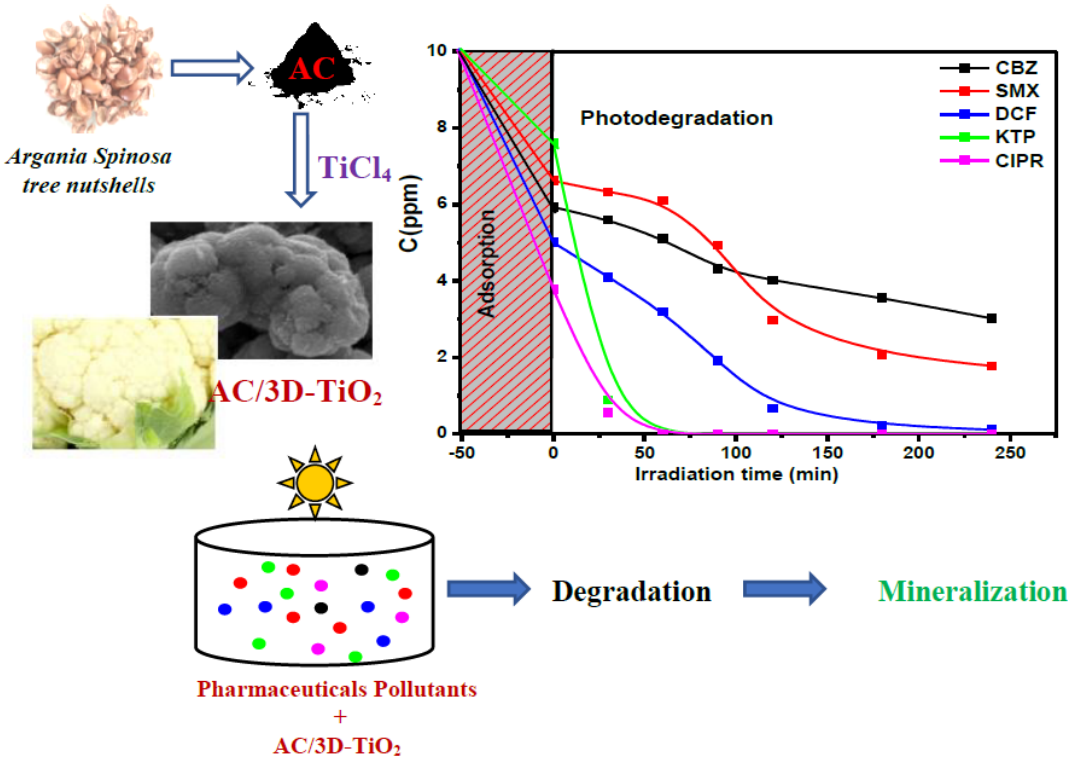

Abstract

The development of advanced photocatalyst for the complete and sustainable removal of emerging organic pollutants such as pharmaceuticals in wastewater is still challenging. Thus, a new three-dimensional cauliflower of TiO_2 immobilized on a bio sourced activated carbon (AC/3D-TiO_2) was successfully synthesized by a hydrothermal method. Its morphological and physicochemical properties were well-characterized with a pure 3D-TiO_2 anatase phase, a high surface area (763 $m^2.g^{-1}$) and a cauliflower-shaped morphology composed of TiO_2 tubes in a radial direction at a micrometric scale. 3D-TiO_2-AC photocatalytic activity on carbamazepine (CBZ), in water showed that around 90% of CBZ elimination is obtained after 4h of exposure, that is 1.5 times more efficient than commercial TiO_2 P25. This was confirmed on five pharmaceuticals (CBZ, ketoprofen, sulfamethoxazole, ciprofloxacin and diclofenac) by

measuring their adsorption, elimination, and mineralization in wastewater highlighting the promising application of AC/3D-TiO_2 in the treatment of wastewaters.

Keywords: Hydrothermal, composite material, titanium dioxide anatase, photocatalysis, adsorption, pharmaceuticals**.**

1. Introduction

Titanium dioxide is considered as the most photoactive photocatalyst that gives the best results in the photodegradation of pollutants in both liquid and gas phases. This is due to its wide band gap (3.2 eV), strong oxidizing power, low cost, non-toxic and high resistance to photo-induced corrosion [1,2]. Thus, it has been widely used in photocatalysis, self-cleaning glass, photovoltaics, sensors, solar energy, paint , textiles, cosmetic, etc.[3].

To date, various strategies have been conducted, such as the control of the crystalline structure, dimensions, and morphology with the purpose of having a very distinguished photocatalytic application and improvement of TiO_2 activity [4–9]. Naturally, TiO_2 exists in three different crystalline phases: anatase, rutile, and brookite. Among these phases, anatase and rutile are the most current ones and it is well known that the anatase phase has the greatest photocatalytic activity compared with others [10,11]. Many studies have proved out that TiO_2 crystals with different phase percentages present a distinguished photocatalytic activity [12,13]. Recently, many researchers focused their efforts to discover a new method that controls the anatase TiO_2 synthesis. Several types of morphology have been prepared, such as nanoflowers, nanorods, nanosheets, nanobelts, nanosphere, nanowires, etc [14–18]. Three-dimensional (3D) nanostructures (e.g., TiO_2 nanosheet spheres or TiO_2 nanorod spheres) have good light absorption capability by permitting more light reflection and multiple scattering inside their structures. They also have the enhanced charge transfer facilitated by 1D or 2D nanostructure, thus retarding the recombination of photogenerated electrons and holes. [17,19,20].

Several methods can be used to prepare TiO_2 anatase such as hydrothermal method [21–23], sol-gel [24–27], electrochemistry [28], chemical vapor deposition [29,30], liquid phase deposition [31] spray deposition [32], and others. The hydrothermal method has been widely used for synthesized the TiO_2 anatase nanostructure because it is simple, inexpensive[33,34]. It is easy to control the shape and size of synthesized nanoparticles with high chemical purity[35–37]. The hydrothermal process provides many possibilities to tune the morphological, optical, and structural properties of TiO_2[38].

This work aims to develop 3D-TiO_2 anatase supported on activated carbon with easy hydrothermal method using $TiCl_4$ as a titanium precursor. Different techniques fully characterized the AC/3D-TiO_2 anatase to assess its morphology, elemental composition, crystal structure, and specific surface area. Its photocatalytic properties were assessed using carbamazepine as a model molecule and compared to a commercial TiO_2 Degussa P25 photocatalyst as a control. An application is carried out on a matrix of five medications (CBZ, SMX, DCF, KTP, and CIPR) in the wastewater of Aix-en-Provence, France, to demonstrate the feasibility of employing AC/3D-TiO_2 to treat a mixture of persistent pharmaceuticals.

2. Material and Methods

2.1 Chemicals

Carbamazepine, ciprofloxacin , sulfamethoxazole, diclofenac and ketoprofen were purchased from Sigma-Aldrich. Hydrochloric acid (37%) and titanium tetrachloride ($TiCl_4$) (99.99%) were provided from Sigma-Aldrich and isopropanol and acetonitrile (HPLC grade) were provided by Fischer Scientific SAS.

2.2 Synthesis AC/3D-TiO_2

The preparation of activated carbon was adopted from previous work described by El Mouchtari et al **[39]**. The AC/3D-TiO_2 composite was prepared by the hydrothermal method. A known amount of $TiCl_4$ (200 µL) was added to 20 mL of a concentrated hydrochloric acid solution (18.5%). After magnetic stirring for 30 min, 1 g of activated carbon was added to the solution and allowed to stir for 30 min. The mixture was transferred to a stainless-steel autoclave, equipped with sealed Teflon® tubes, at 180°C for 16 h under autogenous pressure. After cooling to room temperature (depending on the inertia of the autoclave), the solid was recovered, cleaned several times with distilled water, and dried at 100°C for 24 h. Finally, the material was calcined at 500°C in a muffle furnace for two hours under atmospheric conditions without fresh air regeneration, then washed and dried at 100°C overnight. The 3D-TiO_2 was prepared by the same synthesis method without adding the activated carbon.

2.3 Characterization of AC and AC/3D-TiO_2

The surface morphology of the produced pastes was observed by Scanning Electron Microscopy (SEM) using a FEI Quanta 450 FEG operating at an accelerating voltage

of 200 kV. Thermogravimetric analysis (TGA) was performed in air atmosphere using TGA Q500 (TA 1000) equipment. The specimens (approximately 20 mg) were weight in the platinum crucible. The samples were heated at a rate of 5°C.min^{-1} from ambient temperature to 1000°C. X-ray diffraction patterns were taken at ambient temperature using a Bruker D8 advance diffractometer operating at 20 kV and 10 mA with Cu Kα radiation (k = 1.540593 nm) with a scan speed of 2°min^{-1}. Radials cans were recorded in the reflection scanning mode with 2θ being changed from 5 to 80° with a scan step 0.02°. The data were collected between 5 and 80° in 2θ with a step size of 0.02° at a scanning rate of 5°.min^{-1}. The phase composition of the synthesized products was determined using DIFFRAC.EVA software and PDF-4+2019 database. The measurements of the specific surfaces of the prepared pastes were carried out on an apparatus "A micromeritics 3Flex" by nitrogen adsorption at its liquid temperature (77 K) with previous dry of the samples, and degasification at 100°C for 12 hours. This allows the measurement of the specific surface in the range of 0.01 to >2000 m^2/g and the porosity in the range of 2 to 200 nm.

2.4 Photocatalysis and adsorption experiments

Irradiation was performed with the same system used by EL Mouchtari et al [40–42]. The adsorption capacity of the composite material for CBZ was evaluated in a dark environment at 25°C with a CBZ concentration of 50 mg/L and 0.1g L-1 of AC/3D-TiO_2 anatase cauliflower. Magnetic stirring was used to achieve the adsorption-desorption equilibrium during the experiment (2 h). The residual concentration of CBZ was determined by LC to analyse.

2.5 Application in wastewater

Wastewater was collected from wastewater treatment plant of Aix-en-Provence (Pioline, France), which serves 175 000 inhabitants and operates through primary and biological treatment. The collected wastewater corresponds to the final effluent after the biological treatment. The wastewater was filtered through 0.45 µm membrane filter using Whatman glass microfiber filter, Binder-free GF/C 1.2 µm and immediately stored in the dark at -20°C. Before starting the treatment, we determined the organic and inorganic matter in the wastewater using total organic carbon (TOC) analysis. We found that the water contains 21.79 and 34.66 mg.L^{-1} of organic and inorganic matter, respectively.

50 mg.L^{-1} solutions of each standard have been prepared by dissolving 12.5 mg of each substance in 250 mL of wastewater. The solutions are stored between 0 and 4°C. A solution of the mixture is prepared by diluting the 50 mL mother solutions of ciprofloxacin, carbamazepine, diclofenac sulfamethoxazole and ketoprofen to a mixing concentration of 10 mg.L^{-1}.

2.6 HPLC analysis of pharmaceuticals products (PPs)

The degradation and adsorption monitoring of pharmaceuticals was performed by high-performance liquid chromatography (UPLC Perkin Elmer Altus 30). Chromatographic separation is performed using a Zorbax Eclipse Plus C18 column (3.5 μm; 2.5 × 150 mm) for pharmaceuticals (CBZ, DCF, SMX, CIP, and KTP) distributed by Agilent. The mobile phase flow rate was set at 0.4 mL/min and the oven temperature at 30°C. The gradient is used to elute all pharmaceutical compounds. A 5μL volume of sample is injected into the system using a mobile phase composed of two mixtures acidified with 0.1% (v/v) formic acid (FA): an acetonitrile/water mixture (95/5 v/v) (solvent A) and an acetonitrile/water mixture (5/95 v/v) (solvent B) with the following gradient: Isocratic step at 95% B for 4 min, gradient from 95% to 50% B for 2.5 min, isocratic step at 50% B for 1.5 min, gradient from 50% to 100% B for 1.5 min, isocratic step at 100% B for 1 min.

3. Results and discussion

3.1 Characterization of AC and AC/3D-TiO_2 composites

2.1.1 3D-morphology

SEM images of 3D-TiO_2 (Figure 1) show that this titanium dioxide is composed of deformed balls with quasi-spherical arrangements, designated as a three-dimensional cauliflower-like structure (images a1 and a2). This structure is constituted by an agglomeration of nanometric particles (image a3), as shown in Figure 1.

Furthermore, the images obtained with high resolution show an inside view of the cauliflower structure (image b6), which reveals a three-dimensional growth of TiO_2 in a radial direction at the micrometer scale. When combined with activated carbon, the 3D cauliflower-like morphology was preserved perfectly with an average diameter of 4 micrometers (image b3). On the other hand, the 3D-TiO_2 surface, with a rocky texture

and sharp contours, has undergone a slight alteration forming particles with rounded surface contours (image b6).

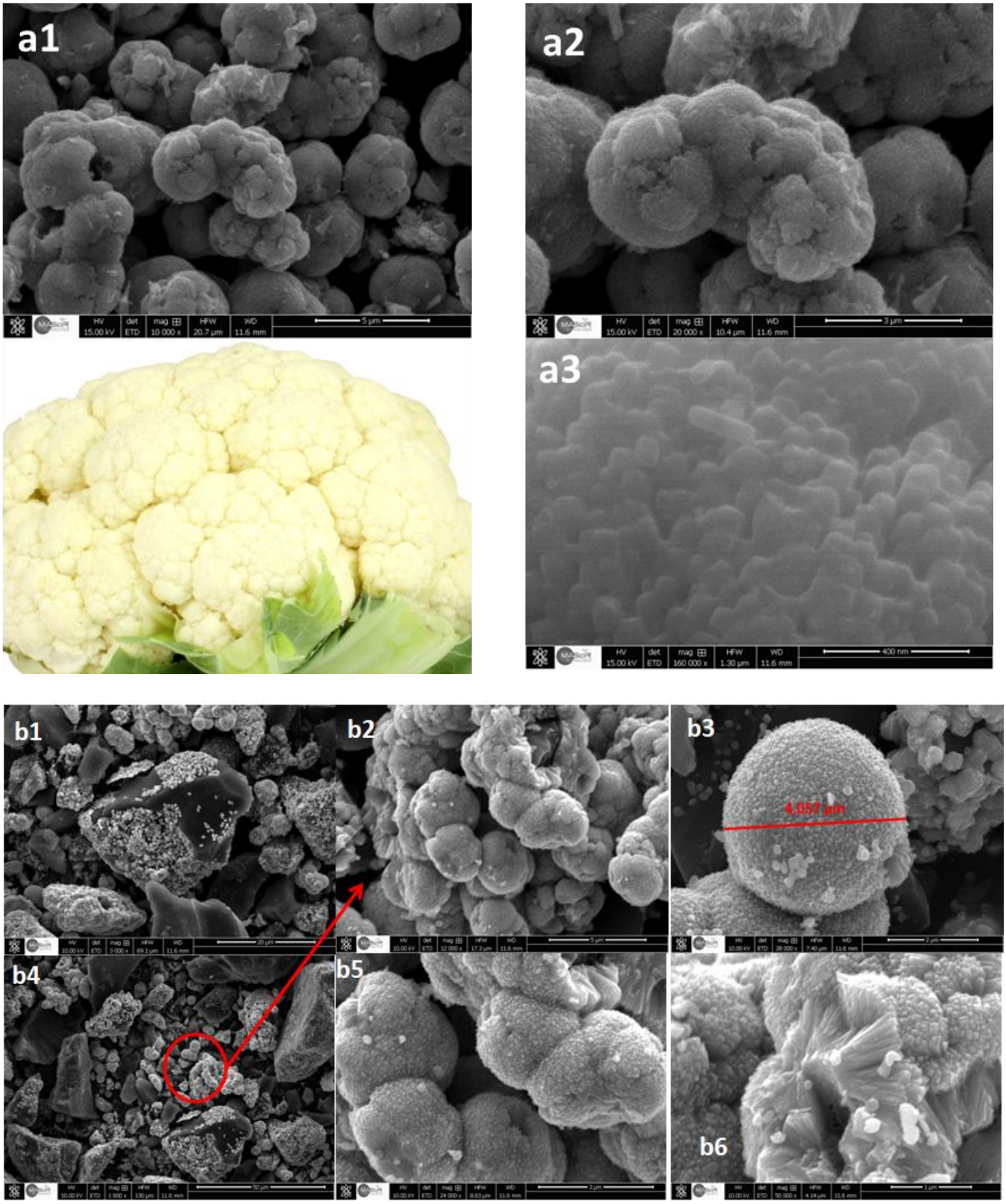

Figure 1. SEM image of 3D-TiO_2 (a) and AC/3D-TiO_2 (b).

3.1.2 Chemical composition

The percentage of 3D-TiO_2 in the prepared composite material has been calculated by thermogravimetric analysis. The thermogram (Figure 2) reveals the presence of two losses of mass. The first one appears between 20 and 100°C with a mass loss of 8.44%, which is due to the loss of water molecules adsorbed on the solid surface. The second stage, between 100 and 1000°C, with a mass loss of 60.16%, corresponds mainly to the combustion of the organic matter of AC as confirmed by AC thermogram. The incomplete thermal decomposition of AC/3D-TiO_2 can only be explained by the residual mineral part of the composite known for its thermal resistance. Based on these results, the 3D-TiO_2 content is equal to 25.22%, which corresponds to the expected percentage.

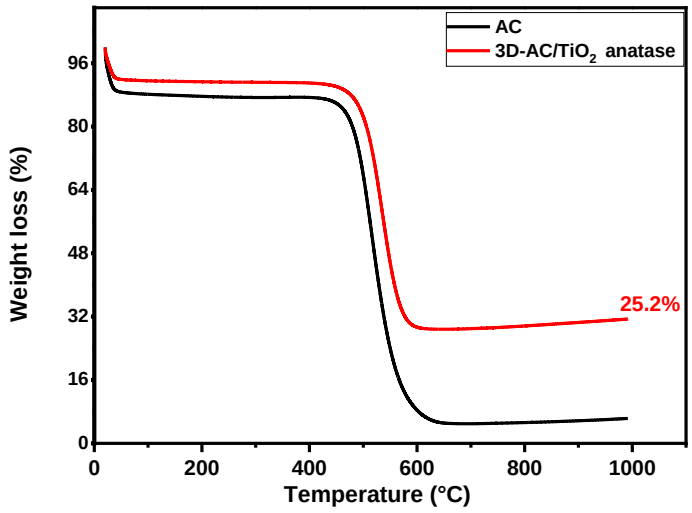

Figure 2. TGA profile of AC and AC/3D-TiO_2.

3.1.3 Crystallography

The X-ray diffractograms of 3D-TiO_2 and AC/3D-TiO_2 are shown in Figure 3. Indeed, the characteristic anatase lines are found at 37.86°, 48.17°, 53.83°, 55.03°, 62.64°, 68.91°, 70.25°, and 75.32° on the diffractograms of titanium dioxide and the composite material. This demonstrates the significant formation of the anatase crystal phase of titanium dioxide in both materials. We found a percentage of the AC/3D-TiO_2 phase composition equal to 100% of the anatase phase with a crystallite size of 50 nm from

the Scherrer relation. These results validate the synthesis route that yields the most photoactive phase [43]. It should be noted that Diffraction peak shapes of TiO_2 in the composite material are wider than those of TiO_2 alone. This gives a very fine particle size, which gives it an important photocatalytic efficiency.

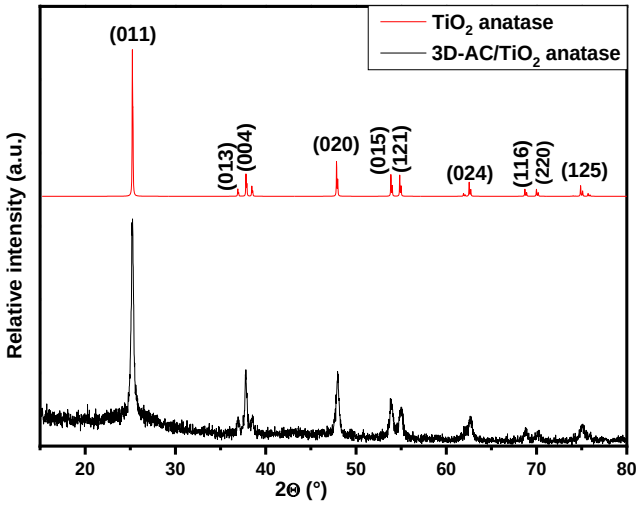

Figure 3. XRD patterns of 3D-TiO_2 and AC/3D-TiO_2 anatase.

3.1.4 Surface area and pore size

From the Figure 4 shows the N_2 adsorption-desorption analyses of activated carbon and composite material AC/3D-TiO_2, AC and composite were determined and are gathered in Table 1.

The AC and 3D-AC/TiO_2 showed that the isotherms correspond to the type I according to IUPAC classification [44], which indicated the presence of microporous on the materials. Concerning surface area values, activated carbon sample displayed a high surface area (1070 $m^2.g^{-1}$) and the mixture with the 3D-TiO_2 decreased the surface area of the composite material (very significantly): pore volume decreased and on the other hand, the diameter of the pores remains constant because the larger size of the 3D-TiO_2 particles (4 µm). This indicates that the immobilization of 3D-TiO_2 on the AC surface has been successfully obtained by hydrothermal method.

Table 1. Textural properties of AC and AC/3D-TiO_2.

Sample	Phase content (%)		Crystalline size (D) (nm)	S_{BET} ($m^2.g^{-1}$)	Pore volume ($cm^3.g^{-1}$)	Pore diameter (nm)
	Anatase	Rutile				
AC	-	-	-	1170	0.59	2.21
AC/3D-TiO_2	100	0	50	763	0.42	2.21

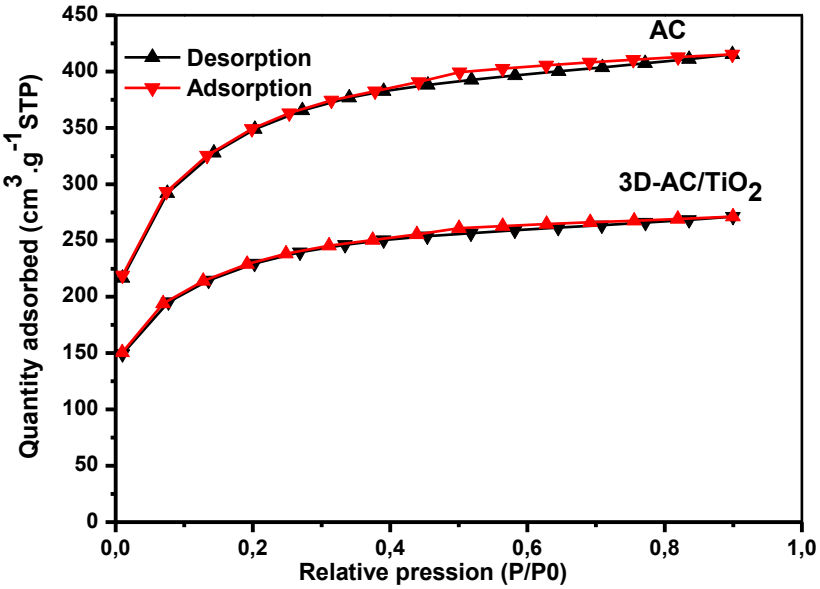

Figure 4. N_2 adsorption/desorption isotherms of AC and AC/3D-TiO_2.

3.2 Adsorption kinetic of carbamazepine on AC/3D-TiO_2

The contact time between the pollutant and the substrate is an important parameter in adsorption treatment. The experiments are carried out at fixed pH (6.5) on 5 mg of AC/3D-TiO_2 and a carbamazepine concentration of 30 $mg.L^{-1}$.

A kinetic study was conducted to determine the contact time required to reach the adsorption equilibrium between the pharmaceutical pollutant molecule and the 3D-AC/3D-TiO_2 material. Figure 5 shows that the adsorption equilibrium is reached after 40 min of contact with a calculated maximum adsorption quantity of about 212 $mg.g^{-1}$.

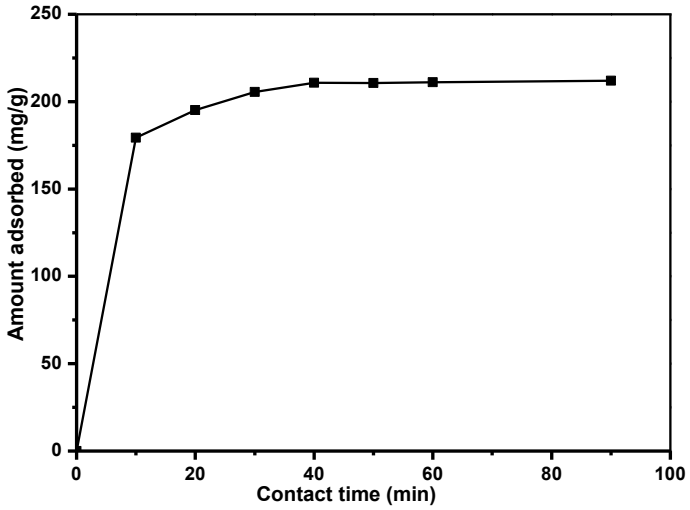

Figure 5. Quantity adsorbed of CBZ on AC/3D-TiO_2 anatase : [CBZ] =30 $mg.L^{-1}$, [AC/3D-TiO_2] = 0.1 $g.L^{-1}$.

The kinetics presented in Figure 5 shows two distinct stages. Efficient adsorption on CBZ takes place in the first minutes of the experiment and an equilibrium sorption state is reached after 40 min of stirring. This rapid adsorption rate is in good agreement with the high specific surface area attributed to its total pore volume (Table 1). Experimental data of carbamazepine adsorption on AC/3D-TiO_2 were adjusted with pseudo first order and pseudo second order using Origin Pro8 as shown in Figure 6.

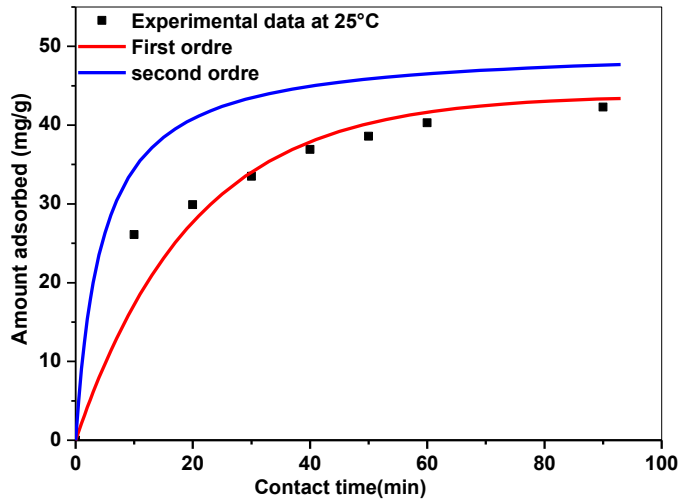

Figure 6. Non-linear pseudo second order and pseudo-first order models for CBZ adsorption on AC/3D-TiO_2 anatase: [CBZ]=5-30$mg.L^{-1}$

Adsorption isotherms describe the interactions between pollutants and adsorbents and are very interesting for an optimization of the adsorption mechanism. The equilibrium relations between adsorbent and adsorbate are described by the adsorption isotherms.

Two widely used mathematical methods of adsorption models, the Langmuir and Freundlich model, have been studied to better understand the mechanism of adsorption of CBZ on the surface of AC and AC/3D-TiO_2. All parameter values and correlation coefficients for both isotherms are presented in table 2.

In order to select the model that best fits the experimental data, we took into account the coefficient of determination (R^2). The table show that the Freundlich model describes satisfactorily the adsorption of CBZ on activated carbon with a coefficient of determination equal to 0.988 and a heterogeneity factor n > 1 which reveals a high adsorption affinity of carbamazepine on activated carbon. This result is in agreement with those obtained by Zirui Yu et al. on the adsorption of two pharmaceuticals (naproxen and carbamazepine) on coconut-based activated carbon [45], which showed that carbamazepine is the most adsorbed compound and that the isotherm is of Freundlich type.

Based on the correlation coefficients (between 0.99 and 0.97) and the values of Q_e(the) calculated by the Langmuir model which are in good agreement with Q_e(exp) (figure 7). The Langmuir model is best suited in our case to describe the monolayer adsorption process of CBZ on our composite compared to Freundlich, indicating the homogeneous nature of AC/3D-TiO_2 sites and pharmaceutical molecules. This model is considered the most appropriate to describe the monolayer adsorption of all PPs on an AC/3D-TiO_2 composite[39,46].

Table 2. Parameter values of CBZ adsorption on AC and AC/3D-TiO_2 using Langmuir and Freundlich model, [CBZ] = 5 to 50 $mg.L^{-1}$, [composite] = 0.1 $g.L^{-1}$, T = 25°C.

Material	**Langmuir model**			**Freundlich model**		
	Q_{max} ($mg.g^{-1}$)	**R^2**	**K_L ($L.mg^{-1}$)**	**K_f $(mg.g^{-1})$ $(mg.L^{-1})^{-n}$**	**R^2**	**1/n**
AC	370	0.988	0.64	181.2	0.995	4.32
AC/3D-TiO_2	250	0.993	0.25	64.7	0.97	0.56

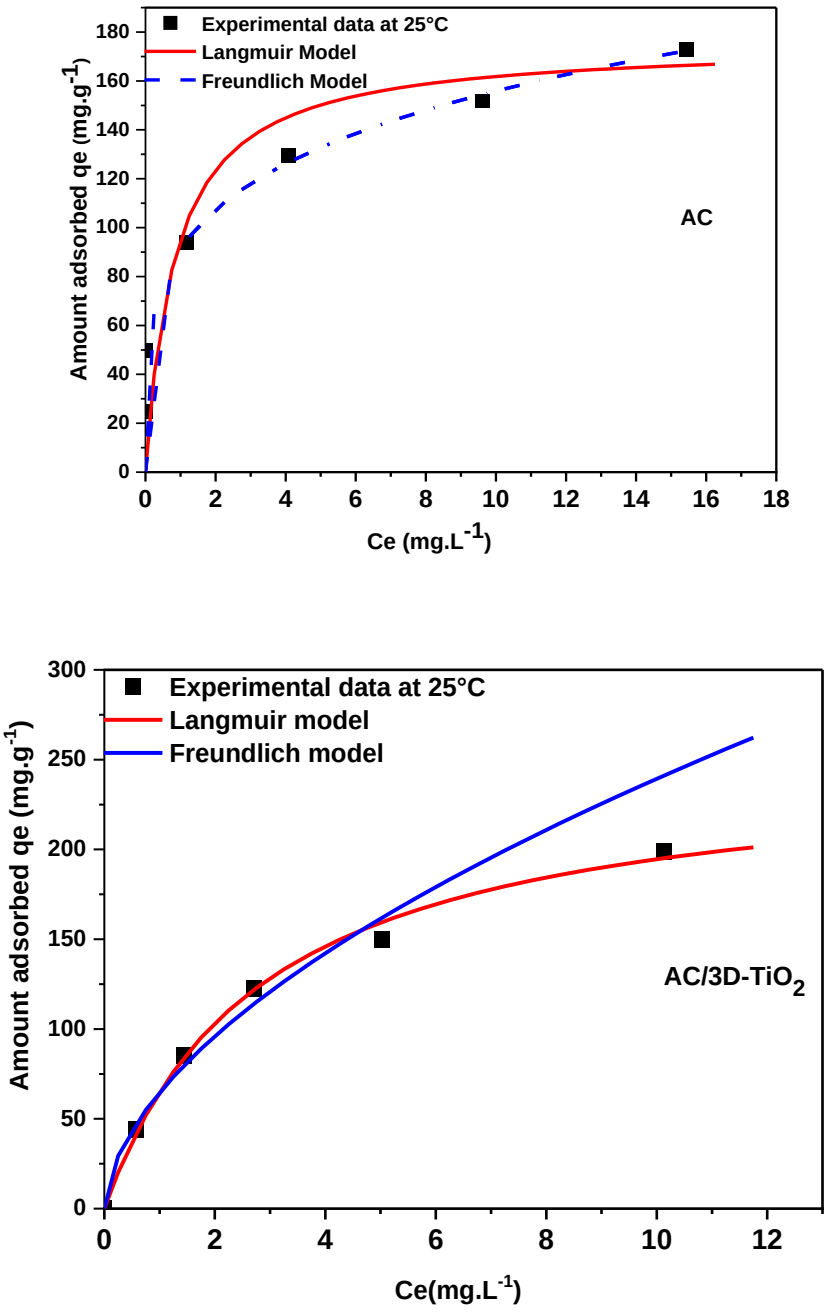

Figure 7. Non-linear Langmuir and Freundlich isotherms obtained for CBZ adsorption on AC and AC/3D-TiO_2 anatase: [CBZ]= 5-30mg.L^{-1}

3.3 Photocatalytic studies

The degradation of the pharmaceutical product by the AC/3D-TiO_2 composite is shown in Figure 8 (blue curve). The photodegradation of the PP was performed after stirring for 50 min in the dark, to reach the adsorption/desorption equilibrium. The percentage of removal in the adsorption process by our composite was about 65%, which proves that the adsorption capacity of AC/3D-TiO_2 is higher than that of naked TiO_2 **[47,48]**.

After the adsorption step, exposure to light in the presence of AC/3D-TiO_2 leads to 70% degradation of carbamazepine in the aqueous solution. These results show that the presence of 3D-TiO_2 deposited on the porous surface of the activated carbon unambiguously enhances the removal of CBZ from the aqueous phase by the chemical photo-induced route. This high reactivity is attributable to the favored transfer of PPs from activated carbon to 3D-TiO_2 particles through the surface diffusion phenomenon that results from the difference in concentration of PPs on AC compared to 3D-TiO_2 [49]. In addition, the possible electron charge density transfer from 3D-TiO_2 to activated carbon at the AC/3D-TiO_2 interface limits the recombination of the electron-hole pair, which increases the production rate of hydroxyl radicals by the photocatalyst [50].

In the presence of the AC/3D-TiO_2 composite, the combined processes of adsorption and photodegradation lead to the efficient removal of CBZ. Other studies have focused on the degradation of pharmaceuticals by AC/TiO_2 composites [51–54]. For example, Gar Alam et al. showed that in the presence of 0.4 $g.L^{-1}$ AC/TiO_2 and under solar irradiation, complete removal of amoxicillin and ampicillin, at an initial concentration of 50 $mg.L^{-1}$, was observed after 180 min of exposure while 85% of diclofenac was transformed under these same conditions [47]. Another similar study on the removal of ibuprofen in the presence of the same composite material (AC/3D-TiO_2) showed that the transformation of 93% of ibuprofen by the adsorption/photocatalysis process with 1.6 $g.L^{-1}$ catalyst under irradiation at 254 nm and after 4 h of irradiation [55]. Although these studies emphasized the effectiveness of the AC/3D-TiO_2 irradiation system, our work shows that the AC/3D-TiO_2 composite provides removal that is more effective with a low catalyst loading (0.1 $g.L^{-1}$), a high drug concentration (50 $mg.L^{-1}$) and a reasonable exposure time of about 4 h.

To identify the reactive species photogenerated and responsible for the degradation of CBZ in AC/3D-TiO_2, two scavengers have been used. Isopropanol (IPA) quenched hydroxyl radicals ($OH^{\cdot}$) and triethanolamine (TEOA) quenched positive holes (h^+) [56–58]. To show these radicals' involvement, a mixture of CBZ and AC/3D-TiO_2 (50 $mg.L^{-1}$ and 0.1$g.L^{-1}$) with 2% v/v IPA or TEOA were irradiated under the same conditions. The effect of oxygen on the degradation of CBZ, was studied by oxygen bubbling before and during the irradiation experiment. The resulting degradation kinetics are shown on figure 8.

The addition of IPA as well as TEOA inhibits the degradation of carbamazepine as no decrease of the concentration was measured during the experiment. The above results suggest that OH radicals were the principal reactive active species in the photocatalytic reaction process, and are generated by the positive holes according to the reaction (1) and (2) [59,60]. On the contrary, there is a total disappearance of the CBZ with oxygen bubbling after 4 hours of irradiation. This implies that O_2 plays an essential role in the degradation of carbamazepine. It enables the generation of superoxide radical $O_2^{\bullet-}$ by reaction 3, which can subsequently produce hydroxyl radicals that are responsible for the degradation of CBZ (reactions 4 and 5). It also participates in slowing down the electron-hole recombination phenomenon, which increases photocatalytic activity [61–63].

$$AC\text{-}TiO_2 + h\upsilon \longrightarrow h^+ + e^- \quad (1)$$

$$h^+ + H_2O \longrightarrow OH^{\cdot} + H^+ \quad (2)$$

$$O_2 + e^- \longrightarrow O_2^{\cdot -} \quad (3)$$

$$O_2^{\cdot -} + H^+ \longrightarrow HO_2^{\cdot} \quad (4)$$

$$HO_2^{\cdot} + e^- + H^+ \longrightarrow 2OH^{\cdot} \quad (5)$$

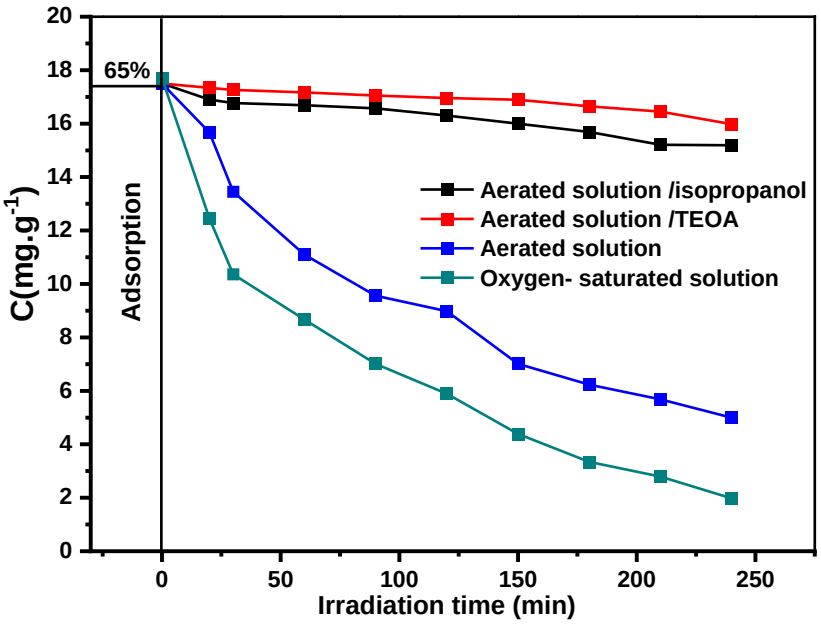

Figure 8. CBZ degradation kinetic in aerated (blue) and oxygen saturated (green) conditions in the presence of isopropanol (black) and TEOA (red), [CBZ]= 50 mg.L^{-1}, [AC/3D-TiO_2] = 0.1 g. L^{-1}, Xe lamp 300W.

The performance of our material synthesized by the hydrothermal method 3D-TiO_2 was compared to the commercial photocatalyst TiO_2 P25. According to the results shown in Figure 9, the degradation of CBZ (25 mg.L^{-1}) by UV-vis light is higher for 3D-TiO_2 than for the commercial photocatalyst TiO_2 P25. The percentage of degradation is about to 86%, while in the case of TiO_2-P25 this percentage is decreased (60%).

Carabin et al. evaluated the removal of carbamazepine in an aqueous solution by a photocatalytic process at 365 nm by TiO_2-P25. The degradation results showed that the percentage of degradation with 1 g.L^{-1} of TiO_2-P25 after 30 min of irradiation and in an acidic medium (pH = 5) is in the same order than our work, as they reach a degradation percentage of 65% [9]. Other work has studied the degradation of CBZ by graphene oxide/TiO_2 (RGOT) under UV light. In a 10 mg.L^{-1} aqueous solution of CBZ, RGOT displayed high adsorption and nearly two-fold higher photodegradation capacity than bare TiO_2, with more than 99 percent CBZ elimination seen within 90 minutes [64]. This study shows the photocatalysis using 3D-TiO_2 is most efficient compared to TiO_2-P25.

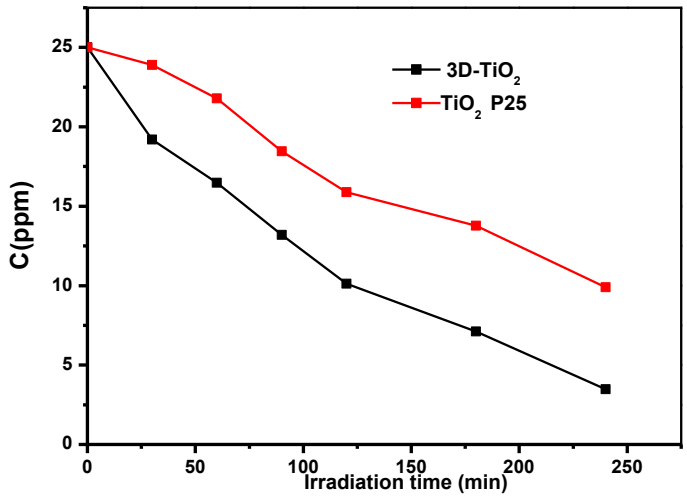

Figure 9. The Comparison between 3D-TiO_2 and TiO_2 P25: [CBZ]=25 mg.L^{-1}, [TiO_2-P25] = 0.4 g. L^{-1}, [3D-TiO_2]=0.1g.L^{-1}, Xe lamp 300W.

3.4 Application in wastewater

An application was realized in the aqueous solution containing a mixture of five pharmaceutical products prepared in a wastewater treatment plant's effluent. First, the direct photolysis of the five pharmaceutical products in wastewater treatment plant water was monitored. The results are illustrated in figure S1. Based on the pollutants' degradation kinetics, under direct excitation, only CBZ was found to be photochemically stable under our experimental conditions. However, approximately 78% DCF, 20% SMX, 90% CIPR, and 99% KTP were degraded in the medium after 4 hours of irradiation.

The photodegradation of PPs was carried out after stirring for 2 hours in the dark to allow the adsorption/desorption equilibrium to be reached. The results illustrated in figure 10, it can be observed the elimination of 40% of CBZ, 50% of DCF, 34% of CIPR and 24% of KTP, and in wastewater effluent, by adsorption process in the presence of AC/3D-TiO_2.

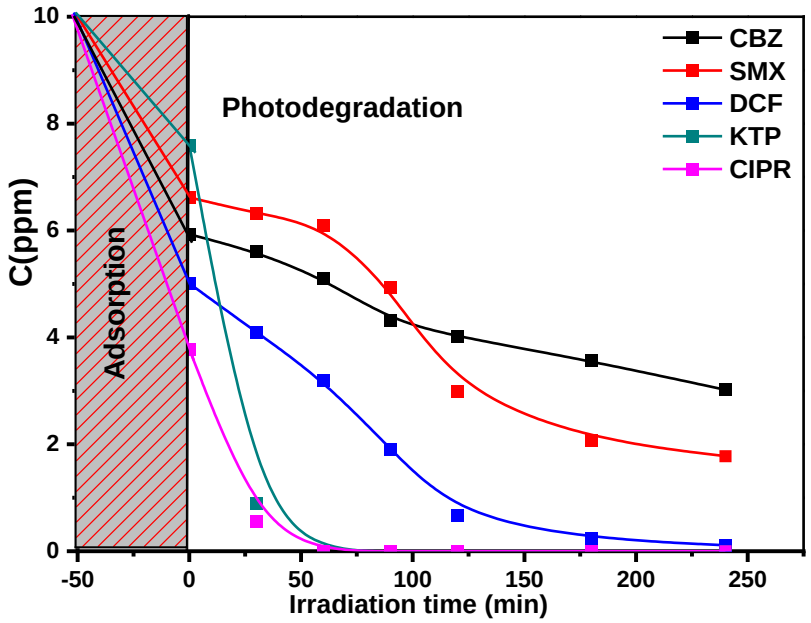

Figure 10. Adsorption and photocatalytic degradation of CBZ, DCF, SMX, KTP and CIPR with AC/3D-TiO_2 from aqueous wastewater of the five products: [AC/3D-TiO_2] = 0.1 $g.L^{-1}$, [PPs] = 10 $mg.L^{-1}$, Xe lamp 300W.

Under irradiation, the adsorption-photodegradation process implies in the removal of PPs mixture from the solution leads to the total disappearance of KTP and CIPR after 60 minutes and 98% of DCF, 73% of SMX, and 50% of CBZ have been eliminated in the solution of wastewater effluent after 4 hours of exposure. These results suggests that the induced degradation process in the presence of AC/TiO_2 3D is involved in CBZ elimination while for the other PPs (DCF, SMX, KTP and CIPR), the contribution of the direct photodegradation pathway should also be considered.

The kinetics of the total mineralization of the five pharmaceuticals was followed in the aqueous phase using the total organic carbon (TOC) analysis (Figure 11). In the presence of AC/3D-TiO_2 and before irradiation, the preliminary step of adsorption leads to the removal of 48% of five pharmaceuticals from the solution. That is to say, 25.9 $mg.L^{-1}$ has transferred to the surface of AC/3D-TiO_2 and the same amount remained in the solution, this concentration was taken as reference. As presented in figure 11, the mineralization of PPs is observed after 4 hours under irradiation at the surface of

AC/3D-TiO_2 but also in the solution even if PPs are not totally degraded (47% degradation).

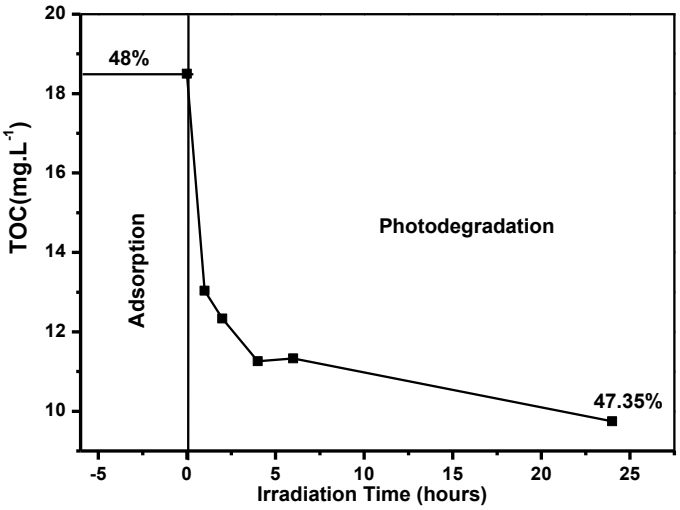

Figure 11. The evolution of TOC as a function of irradiation time in aqueous, [PPs] = 50 $mg.L^{-1}$, [AC/3D-TiO_2] = 0.1$g.L^{-1}$, Xe 300 W, aerated conditions

4. Conclusion

In summary, a 3D cauliflower-like TiO_2 has been successfully immobilized on a bio sourced activated carbon using hydrothermal method leading to a bio composite with very interesting properties: new 3D morphology, large surface area and exclusive photoactive anatase structure. In addition, AC/3D-TiO_2 material proved its ability to efficiently adsorb pharmaceuticals, induce their degradation and mineralization by photocatalysis in pure water and wastewater. This result shows that this material represents a promising and economically sustainable solution for water depollution.

Compliance with ethical standards

Competing Interest

There are no conflicts of interest to declare.

References

[1] T.L. Thompson, J.T. Yates, Surface Science Studies of the Photoactivation of TiO_2 New Photochemical Processes, Chemical Reviews. **106** 4428–4453 (2006). doi: 10.1021/cr050172k.

[2] M. Pal, J. García Serrano, P. Santiago, U. Pal, Size-Controlled Synthesis of Spherical TiO_2 Nanoparticles: Morphology, Crystallization, and Phase Transition, The Journal of Physical Chemistry C. **111** 96–102 (2007). doi: 10.1021/jp0618173.

[3] X. Chen, S.S. Mao, Titanium Dioxide Nanomaterials: Synthesis, Properties, Modifications, and Applications, Chemical Reviews. **107** 2891–2959 (2007). doi: 10.1021/cr0500535.

[4] T.-L.T. Le, T.-H.T. Le, K. Nguyen Van, H. Van Bui, T.G. Le, V. Vo, Controlled growth of TiO_2 nanoparticles on graphene by hydrothermal method for visible-light photocatalysis, Journal of Science: Advanced Materials and Devices. **6** 516–527 (2021). doi: 10.1016/j.jsamd.2021.07.003.

[5] A.O. Özdemir, B. Caglar, O. Çubuk, F. Coldur, M. Kuzucu, E.K. Guner, B. Doğan, S. Caglar, K.V. Özdokur, Facile synthesis of TiO_2-coated cotton fabric and its versatile applications in photocatalysis, pH sensor and antibacterial activities, Materials Chemistry and Physics. **287** 126342 (2022). doi: 10.1016/j.matchemphys.2022.126342.

[6] S. Kumar, Bhawna, R. Sharma, A. Gupta, K.K. Dubey, A.M. Khan, R. Singhal, R. Kumar, A. Bharti, P. Singh, R. Kant, V. Kumar, TiO2 based photocatalysis membranes: An efficient strategy for pharmaceutical mineralization, Science of The Total Environment. 157221(2022). doi: 0.1016/j.scitotenv.2022.157221.

[7] B. Regraguy, M. Rahmani, J. Mabrouki, F. Drhimer, I. Ellouzi, C. Mahmou, A. Dahchour, M.E. Mrabet, S.E. Hajjaji, Photocatalytic degradation of methyl orange in the presence of nanoparticles NiSO4/TiO2, Nanotechnol. Environ. Eng. **7** 157–171 (2022). doi: 10.1007/s41204-021-00206-0.

[8] Y. Cheng, J. Gao, Q. Shi, Z. Li, W. Huang, In situ electrochemical reduced Au loaded black TiO2 nanotubes for visible light photocatalysis, Journal of Alloys and Compounds. **901** 163562 (2022). doi: 10.1016/j.jallcom.2021.163562.

[9] R. Atchudan, T.N. Jebakumar Immanuel Edison, S. Perumal, D. Karthikeyan, Y.R. Lee, Effective photocatalytic degradation of anthropogenic dyes using graphene oxide grafting titanium dioxide nanoparticles under UV-light irradiation, Journal of Photochemistry and Photobiology A: Chemistry. **333** 92–104 (2017). doi: 10.1016/j.jphotochem.2016.10.021.

[10] M. Hamandi, G. Berhault, C. Guillard, H. Kochkar, Influence of reduced graphene oxide on the synergism between rutile and anatase TiO_2 particles in photocatalytic degradation of formic acid, Molecular Catalysis. **432** (2017) 125–130 (2017). DOI:10.1016/j.mcat.2017.01.003.

[11] S.K. Shahi, N. Kaur, S. Sandhu, J.S. Shahi, V. Singh, Influences of a new templating agent on the synthesis of coral-like TiO_2 nanoparticles and their photocatalytic activity, Journal of Science: Advanced Materials and Devices. **2** 347–353 (2017). doi: 10.1016/j.jsamd.2017.07.006.

[12] Y.K. Kho, A. Iwase, W.Y. Teoh, L. Mädler, A. Kudo, R. Amal, Photocatalytic H_2 Evolution over TiO_2 Nanoparticles. The Synergistic Effect of Anatase and Rutile, The Journal of Physical Chemistry C. **114** 2821–2829 (2010). doi:10.1021/jp910810r.

[13] F. Xu, W. Xiao, B. Cheng, J. Yu, Direct Z-scheme anatase/rutile bi-phase nanocomposite TiO_2 nanofiber photocatalyst with enhanced photocatalytic H 2 -production activity, International Journal of Hydrogen Energy. **39** 15394–15402 (2014). doi:10.1016/j.ijhydene.2014.07.166.

[14] Z. Li, Z. Ren, Y. Qu, S. Du, J. Wu, L. Kong, G. Tian, W. Zhou, H. Fu, Hierarchical N-Doped TiO_2 Microspheres with Exposed (001) Facets for Enhanced Visible Light Catalysis:

Hierarchical N-Doped TiO_2 Microspheres, European Journal of Inorganic Chemistry. **2014** 2146–2152 (2014). doi: 10.1002/ejic.201301561.
[15] Y. Jiang, M. Li, D. Song, X. Li, Y. Yu, A novel 3D structure composed of strings of hierarchical TiO2 spheres formed on TiO_2 nanobelts with high photocatalytic properties, Journal of Solid State Chemistry. **211** 90–94 (2014). doi:10.1016/j.jssc.2013.12.002.
[16] J. Yu, J. Fan, K. Lv, Anatase TiO2 nanosheets with exposed (001) facets: improved photoelectric conversion efficiency in dye-sensitized solar cells, Nanoscale. **2** 2144(2010). doi: 10.1039/c0nr00427h.
[17] Y. Jiang, M. Li, D. Song, X. Li, Y. Yu, A novel 3D structure composed of strings of hierarchical TiO2 spheres formed on TiO_2 nanobelts with high photocatalytic properties, Journal of Solid State Chemistry. **211** 90–94 (2014). doi: 10.1016/j.jssc.2013.12.002.
[18] M. Ge, C. Cao, J. Huang, S. Li, Z. Chen, K.-Q. Zhang, S.S. Al-Deyab, Y. Lai, A review of one-dimensional TiO_2 nanostructured materials for environmental and energy applications, Journal of Materials Chemistry A. **4** 6772–6801 (2016). doi: 10.1039/C5TA09323F.
[19] G. Ai, W.-T. Sun, Y.-L. Zhang, L.-M. Peng, Nanoparticle and nanorod TiO_2 composite photoelectrodes with improved performance, Chemical Communications. **47** 6608 (2011). doi:10.1039/c1cc11092f.
[20] W.-Q. Wu, B.-X. Lei, H.-S. Rao, Y.-F. Xu, Y.-F. Wang, C.-Y. Su, D.-B. Kuang, Hydrothermal Fabrication of Hierarchically Anatase TiO_2 Nanowire arrays on FTO Glass for Dye-sensitized Solar Cells, Scientific Reports. **3** (2013). doi:10.1038/srep01352.
[21] G. Shilpa, P. Mohan Kumar, D. Kishore Kumar, P.R. Deepthi, A. Sukhdev, P. Bhaskar, A rutile phase-TiO_2 film via a facile hydrothermal method for photocatalytic methylene blue dye decolourization, Materials Today: Proceedings. **62** 5477–5482 (2022). https://doi.org/10.1016/j.matpr.2022.04.148.
[22] Manisha, V. Kumar, D. Kumar Sharma, Fabrication of dimensional hydrophilic TiO_2 nanostructured surfaces by hydrothermal method, Materials Today: Proceedings. 46 2171–2174 (2021). doi: 10.1016/j.matpr.2021.02.690.
[23] R. Atchudan, T.N.J.I. Edison, S. Perumal, R. Vinodh, Y.R. Lee, In-situ green synthesis of nitrogen-doped carbon dots for bioimaging and TiO2 nanoparticles@nitrogen-doped carbon composite for photocatalytic degradation of organic pollutants, Journal of Alloys and Compounds. **766** 12–24 (2018). doi: 10.1016/j.jallcom.2018.06.272.
[24] S.M. Hassan, A.I. Ahmed, M.A. Mannaa, Preparation and characterization of SnO2 doped TiO2 nanoparticles: Effect of phase changes on the photocatalytic and catalytic activity, Journal of Science: Advanced Materials and Devices. **4** 400–412 (2019). doi: 10.1016/j.jsamd.2019.06.004.
[25] T. Ghrib, N.K. AL-Saleem, A. AL-Naghmaish, A.A. Elshekhipy, S. Brini, K. Briki, K.A. Elsayed, Annealing effect on the microstructural, optical, electrical, and thermal properties of $Cu_2O/TiO_2/Cu_2O/TiO_2$/Si heterojunction prepared by sol-gel technique, Micro and Nanostructures. 164 107119 (2022). doi: 10.1016/j.spmi.2021.107119.
[26] W. Nachit, H. Ait Ahsaine, Z. Ramzi, S. Touhtouh, I. Goncharova, K. Benkhouja, Photocatalytic activity of anatase-brookite TiO_2 nanoparticles synthesized by sol gel method at low temperature, Optical Materials. **129** 112256 (2022). doi:10.1016/j.optmat.2022.112256.
[27] O. Sadek, S. Touhtouh, M. Rkhis, R. Anoua, M. El Jouad, F. Belhora, A. Hajjaji, Synthesis by sol-gel method and characterization of nano-TiO_2 powders, Materials Today: Proceedings. (2022) S2214785322044005. doi: 10.1016/j.matpr.2022.06.385.

[28] Y. Li, W. Zhang, X. Shen, P. Peng, L. Xiong, Y. Yu, Octahedral Cu_2O-modified TiO_2 nanotube arrays for efficient photocatalytic reduction of CO_2, Chinese Journal of Catalysis. **36** 2229–2236 (2015). doi: 10.1016/S1872-2067(15)60991-3.
[29] H.-Y. Liu, Y.-L. Hsu, Y.-X. Zheng, Investigation of oxygen deficiency-rich/oxygen deficiency-poor stacked TiO_2 based resistive random access memory by mist chemical vapor deposition, Ceramics International. S0272884222011804 (2022). doi: 10.1016/j.ceramint.2022.04.038.
[30] D. Bijou, E. Wagner, W. Maudez, T. Cornier, M. Yettou, G. Benvenuti, S. Daniele, Study of titanium amino-alkoxide derivatives as TiO_2 Chemical Beam Vapour Deposition precursor, Materials Chemistry and Physics. **277** 125561 (2022). doi:10.1016/j.matchemphys.2021.125561.
[31] J.-G. Yu, H.-G. Yu, B. Cheng, X.-J. Zhao, J.C. Yu, W.-K. Ho, The Effect of Calcination Temperature on the Surface Microstructure and Photocatalytic Activity of TiO_2 Thin Films Prepared by Liquid Phase Deposition, The Journal of Physical Chemistry B. 107 13871–13879 (2003). doi: 10.1021/jp036158y.
[32] W. Naffouti, A. Jrad, T. Ben Nasr, S. Ammar, N. Turki-Kamoun, Structural, morphological and optical properties of TiO_2:Mn thin films prepared by spray pyrolysis technique, Journal of Materials Science: Materials in Electronics. **27** 4622–4630 (2016). doi:10.1007/s10854-016-4339-2.
[33] J. Cabrera, H. Alarcón, A. López, R. Candal, D. Acosta, J. Rodriguez, Synthesis, characterization and photocatalytic activity of 1D TiO_2 nanostructures, Water Science and Technology**. 70** 972–979 (2014).doi: 10.2166/wst.2014.312.
[34] J.-N. Nian, H. Teng, Hydrothermal Synthesis of Single-Crystalline Anatase TiO_2 Nanorods with Nanotubes as the Precursor, J. Phys. Chem. B. **110** 4193–4198 (2006). doi:10.1021/jp0567321.
[35] A.H. Mamaghani, F. Haghighat, C.-S. Lee, Hydrothermal/solvothermal synthesis and treatment of TiO_2 for photocatalytic degradation of air pollutants: Preparation, characterization, properties, and performance, Chemosphere. **219** 804–825 (2019). doi: 10.1016/j.chemosphere.2018.12.029.
[36] R. Katal, S. Masudy-Panah, M. Tanhaei, M.H.D.A. Farahani, H. Jiangyong, A review on the synthesis of the various types of anatase TiO_2 facets and their applications for photocatalysis, Chemical Engineering Journal. **384** 123384 (2020). doi:10.1016/j.cej.2019.123384.
[37] X. Wang, Z. Li, J. Shi, Y. Yu, One-Dimensional Titanium Dioxide Nanomaterials: Nanowires, Nanorods, and Nanobelts, Chem. Rev. **114** 9346–9384 (2014). doi:10.1021/cr400633s.
[38] R. Hidayat, G. Fadillah, S. Wahyuningsih, A control of TiO_2 nanostructures by hydrothermal condition and their application: a short review, IOP Conf. Ser.: Mater. Sci. Eng**. 578** 012031(2019). doi:10.1088/1757-899X/578/1/012031.
[39] E.M. El Mouchtari, C. Daou, S. Rafqah, F. Najjar, H. Anane, A. Piram, A. Hamade, S. Briche, P. Wong-Wah-Chung, TiO_2 and activated carbon of Argania Spinosa tree nutshells composites for the adsorption photocatalysis removal of pharmaceuticals from aqueous solution, Journal of Photochemistry and Photobiology A: Chemistry. **388** 112183 (2020). doi:10.1016/j.jphotochem.2019.112183.
[40] E.M. El Mouchtari, C. Daou, S. Rafqah, F. Najjar, H. Anane, A. Piram, A. Hamade, S. Briche, P. Wong-Wah-Chung, TiO_2 and activated carbon of Argania Spinosa tree nutshells composites for the adsorption photocatalysis removal of pharmaceuticals from aqueous solution, Journal of Photochemistry and Photobiology A: Chemistry. **388** 112183 (2020). doi:10.1016/j.jphotochem.2019.112183.
[41] E.M. El Mouchtari, L. Bahsis, L. El Mersly, H. Anane, S. Lebarillier, A. Piram, S. Briche, P. Wong-Wah-Chung, S. Rafqah, Insights in the Aqueous and Adsorbed Photocatalytic

Degradation of Carbamazepine by a Biosourced Composite: Kinetics, Mechanisms and DFT Calculations, Int J Environ Res. **15** 135–147 (2021). doi: 10.1007/s41742-020-00300-2.

[42] E.M. El Mouchtari, M. Claeys-Bruno, S. Rafqah, D. Manzon, H. Anane, S. Lebarillier, A. Piram, S. Briche, P. Wong-Wah-Chung, Optimisation of a photocatalytic water treatment using response surface methodology and quality by design Approach, International Journal of Environmental Analytical Chemistry. **102** 1–17 (2022). doi: 10.1080/03067319.2021.2012171.

[43] M. Peñas-Garzón, A. Gómez-Avilés, C. Belver, J.J. Rodriguez, J. Bedia, Degradation pathways of emerging contaminants using TiO_2-activated carbon heterostructures in aqueous solution under simulated solar light, Chemical Engineering Journal. **392** 124867 (2020). doi:10.1016/j.cej.2020.124867.

[44] K.S.W. Sing, Reporting physisorption data for gas/solid systems with special reference to the determination of surface area and porosity (Recommendations 1984), Pure and Applied Chemistry. **57** 603–619(1985). doi:0.1351/pac198557040603.

[45] Z. Yu, S. Peldszus, P.M. Huck, Adsorption characteristics of selected pharmaceuticals and an endocrine disrupting compound—Naproxen, carbamazepine and nonylphenol—on activated carbon, Water Research. **42** 2873–2882 (2008). doi:10.1016/j.watres.2008.02.020.

[46] V. Calisto, C.I.A. Ferreira, J.A.B.P. Oliveira, M. Otero, V.I. Esteves, Adsorptive removal of pharmaceuticals from water by commercial and waste-based carbons, Journal of Environmental Management. **152** 83–90(2015). doi:10.1016/j.jenvman.2015.01.019.

[47] M. Gar Alalm, A. Tawfik, S. Ookawara, Enhancement of photocatalytic activity of TiO2 by immobilization on activated carbon for degradation of pharmaceuticals, Journal of Environmental Chemical Engineering. **4** 1929–1937(2016). doi:10.1016/j.jece.2016.03.023.

[48] Q.-S. Liu, T. Zheng, P. Wang, J.-P. Jiang, N. Li, Adsorption isotherm, kinetic and mechanism studies of some substituted phenols on activated carbon fibers, Chemical Engineering Journal. **157** 348–356 (2010).doi:10.1016/j.cej.2009.11.013.

[49] T.S. Jamil, M.Y. Ghaly, N.A. Fathy, T.A. Abd el-halim, L. Österlund, Enhancement of TiO2 behavior on photocatalytic oxidation of MO dye using TiO_2/AC under visible irradiation and sunlight radiation, Separation and Purification Technology. **98** 270–279(2012). doi:10.1016/j.seppur.2012.06.018.

[50] E. Carpio, P. Zúñiga, S. Ponce, J. Solis, J. Rodriguez, W. Estrada, Photocatalytic degradation of phenol using TiO_2 nanocrystals supported on activated carbon, Journal of Molecular Catalysis A: Chemical. **228** 293–298(2005). doi:10.1016/j.molcata.2004.09.066.

[51] Patiparn Punyapalakul, Thitikamon Sitthisorn, Removal Of Ciprofloxazin And Carbamazepine By Adsorption On Functionalized Mesoporous Silicates, (2010). doi:10.5281/ZENODO.1062550.

[52] H. Khazri, I. Ghorbel-Abid, R. Kalfat, M. Trabelsi-Ayadi, Removal of ibuprofen, naproxen and carbamazepine in aqueous solution onto natural clay: equilibrium, kinetics, and thermodynamic study, Appl Water Sci. **7** 3031–3040(2017). doi:10.1007/s13201-016-0414-3.

[53] R. Meribout, Y. Zuo, A.A. Khodja, A. Piram, S. Lebarillier, J. Cheng, C. Wang, P. Wong-Wah-Chung, Photocatalytic degradation of antiepileptic drug carbamazepine with bismuth oxychlorides (BiOCl and BiOCl/AgCl composite) in water: Efficiency evaluation and elucidation degradation pathways, Journal of Photochemistry and Photobiology A: Chemistry. **328** 105–113(2016). doi:10.1016/j.jphotochem.2016.04.024.

[54] S.K. Alharbi, J. Kang, L.D. Nghiem, J.P. van de Merwe, F.D.L. Leusch, W.E. Price, Photolysis and UV/H_2O_2 of diclofenac, sulfamethoxazole, carbamazepine, and

trimethoprim: Identification of their major degradation products by ESI–LC–MS and assessment of the toxicity of reaction mixtures, Process Safety and Environmental Protection. **112**222–234 (2017). doi:10.1016/j.psep.2017.07.015.
[55] Y. Gu, J. Yperman, R. Carleer, J. D'Haen, J. Maggen, S. Vanderheyden, K. Vanreppelen, R.M. Garcia, Adsorption and photocatalytic removal of Ibuprofen by activated carbon impregnated with TiO_2 by UV–Vis monitoring, Chemosphere. **217** 724–731 (2019). doi:10.1016/j.chemosphere.2018.11.068.
[56] K.D. Asmus, H. Moeckel, A. Henglein, Pulse radiolytic study of the site of hydroxyl radical attack on aliphatic alcohols in aqueous solution, The Journal of Physical Chemistry. **77** 1218–1221(1973). https://doi.org/10.1021/j100629a007.
[57] S.C. Yan, Z.S. Li, Z.G. Zou, Photodegradation of Rhodamine B and Methyl Orange over Boron-Doped g-C_3N_4 under Visible Light Irradiation, Langmuir. **26** 3894–3901 (2010). doi:10.1021/la904023j.
[58] S.-H. Yoon, J.H. Lee, Oxidation Mechanism of As(III) in the UV/TiO_2 System: Evidence for a Direct Hole Oxidation Mechanism, Environmental Science & Technology. **39** (2005) 9695–9701. doi:10.1021/es051148r.
[59] Z. Zhu, H. Cai, D.-W. Sun, Titanium dioxide (TiO_2) photocatalysis technology for nonthermal inactivation of microorganisms in foods, Trends in Food Science & Technology. **75** 23–35(2018).doi:10.1016/j.tifs.2018.02.018.
[60] M.R. Al-Mamun, S. Kader, M.S. Islam, M.Z.H. Khan, Photocatalytic activity improvement and application of UV-TiO_2 photocatalysis in textile wastewater treatment: A review, Journal of Environmental Chemical Engineering. **7** 103248 (2019). doi:10.1016/j.jece.2019.103248.
[61] W. Xue, H. Sun, X. Hu, X. Bai, J. Fan, E. Liu, UV-VIS-NIR-induced extraordinary H2 evolution over W18O49/Cd0.5Zn0.5S: Surface plasmon effect coupled with S-scheme charge transfer, Chinese Journal of Catalysis. **43** 234–245 (2022). doi: 10.1016/S1872-2067(20)63783-4.
[62] H. Gerischer, A. Heller, The role of oxygen in photooxidation of organic molecules on semiconductor particles, J. Phys. Chem. **95** 5261–5267 (1991). doi: 10.1021/j100166a063.
[63] S.X. Liu, X.Y. Chen, X. Chen, A TiO_2/AC composite photocatalyst with high activity and easy separation prepared by a hydrothermal method, Journal of Hazardous Materials. **143** 257–263 (2007). https://doi.org/10.1016/j.jhazmat.2006.09.026.
[64] M. Nawaz, W. Miran, J. Jang, D.S. Lee, One-step hydrothermal synthesis of porous 3D reduced graphene oxide/TiO2 aerogel for carbamazepine photodegradation in aqueous solution, Applied Catalysis B: Environmental. **203** 85–95 (2017). doi:10.1016/j.apcatb.2016.10.007.